

Efficient Waveform Design for High-Bit-Rate W-band Satellite Transmissions

Claudio Sacchi *IEEE Senior Member* (*), Tommaso Rossi (**), Marina Ruggieri *IEEE Senior Member* (**), and Fabrizio Granelli *IEEE Senior Member* (*)

(*) University of Trento, Department of Information Engineering and Computer Science (DISI), Via Sommarive 14, I-38050, Trento (Italy), e-mail: sacchi@disi.unitn.it, granelli@disi.unitn.it

(**) University of Rome Tor Vergata, Department of Electronic Engineering, Via del Politecnico 1, I-00133, Rome (Italy) e-mail: tommaso.rossi@uniroma2.it, ruggieri@uniroma2.it

Abstract

In the EHF (Extremely High Frequency) domain, W-band (75-110 GHz) offers promising perspectives for future satellite communications, mainly in terms of large bandwidth availability for high-bit-rate transmission. In this work¹, an innovative physical (PHY) layer design for broadband satellite connections operating in W-band is proposed, which is based on the Prolate Spheroidal Wave Functions (PSWFs). PSWF waveforms (originally proposed in short-range indoor Ultra Wideband (UWB) communications) are aimed at optimizing the tradeoff between the concentration of pulse energy in a finite time interval and in a limited bandwidth. In our paper, PSWF-based 4-ary PSM modulation, characterized by a near-optimal compromise between spectral and envelope compactness, has been tested for the radio interface of a W-band geostationary (GEO) downlink connection. The effect of nonlinear distortions, introduced by power-efficient saturating amplifiers, can be drastically reduced without any power back-off and maintaining a very good spectral efficiency. Experimental results, obtained by means of realistic simulations, fully demonstrate the potential advantages taken by PSWF in terms of increased spectral efficiency, link availability and net payload rate with respect to state-of-the-art pulse-shaped modulations (raised-cosine filtered QAM and Gaussian Minimum Shift Keying), commonly employed in satellite communications.

Index Terms— Satellite communications, EHF, UWB, Prolate Spheroidal Wave Functions, nonlinear distortions, pulse shaping.

Corresponding author:

Claudio Sacchi

PhD, assistant professor

University of Trento, Dept. of Information Engineering and Computer Science (DISI)

Via Sommarive 14, I-38050, Trento (Italy)

Phone: +39-0461-883907, Fax: +39-0461-882093

E-mail: sacchi@disi.unitn.it

¹ A preliminary abbreviated version of this paper has been published at the IEEE EHF-AERCOMM Workshop co-located with IEEE Globecom 2008 Conference, New Orleans, Nov. 30 – Dec. 4, 2008.

1. Introduction

The future exploitation of Extremely High Frequencies (EHF) for broadband aerospace communications will generate critical challenges to designers and developers. The claimed objective is to reach the so-called “gigabit connectivity” in order to make such a radio segment a potential “backbone on the air” for global wireless connectivity [1]. Such objective is not realistically achievable by exploiting currently saturated bandwidth portions (Ku and Ka bands). For this reason, the push towards higher frequencies will characterize future R&D on satellite communications [2]. Recently, some proposals for the exploitation of Q/V-bands (31-60 GHz) and W-band (75-110 GHz) in satellite communications are being issued [3]. W-band seems to provide a favorable “attenuation window” related to Oxygen absorption (values around 0.05 dB/km [4]). In addition, W-band is still scarcely used for data transmission (only analog radar applications are supported in those frequencies [3]) and, therefore, interference level is very low. For these reasons, despite the increasing attenuation due to rain, water vapor and clouds, W-band is regarded as a good candidate for supporting future broadband services in the millimeter wave domain. The experimentation of W-band for data transmission is currently in a very early stage. In recent years, Italian Space Agency (ASI) issued two “startup experiments” proposed by Ruggieri et. al.: DAVID-DCE (Digital Audio-Video Interactive Distribution – Data Collection Experiment) [3] [5] and WAVE (W-band Analysis and evaluation) [6] [7].

Preliminary on-going experimentations evidenced the actual possibility of exploiting W-band for broadband connections at very high data rates. Nevertheless, some areas of uncertainty and risk can hinder the efficient exploitation of these large and almost interference-free bandwidth portions. These are related to: a) non-idealities of

communication payloads (phase-noise, linear and nonlinear distortions, timing uncertainties etc.) [8] and b) lack of knowledge of signal propagation modalities in W-band. PHY-layer design should carefully take into account all these problems in order to provide the desired quality of service. The analysis of requirements of an efficient W-band satellite PHY-layer should start from some known issues that can be listed as follows [8]:

- 1) heavy pathloss due to high carrier frequency;
- 2) presence of nonlinear distortions due to the necessity of using amplifiers at the maximum level of power efficiency (W-band power resources are quite scarce and should be intensively exploited);
- 3) presence of time and frequency uncertainties (symbol unbalance, phase noise) that become increasingly relevant as the data rate grows;
- 4) finite system passband and nonideal bandpass characterization of the satellite system (presence of linear distortion);
- 5) spectrum management issues related to the presence of other transmitters exploiting adjacent bandwidth portions (in practical satellite applications, bandwidth resources are always limited and spectrum is always shared by a variety of users).

The idea of obtaining gigabit connectivity by means of W-band LEO (Low Earth Orbit) satellites has been preliminarily explored by Sacchi and Grigorova in [9] by considering the use of multi-level TCM (Trellis Code Modulation). The study of [9] analyzed the effects of nonlinear distortion and phase noise on TCM, assuming the ideal hypothesis of unlimited bandwidth availability and considering the use of rectangular pulse as digital waveform. It is known that rectangular pulses are unlimited in bandwidth with high-power sidelobes. Therefore, the resulting modulated signal would span its bandwidth over a very large frequency range with

relevant power level measured outside the main spectral lobe. Considering that satellite channels are closely located, adjacent channel interference (ACI) would become a major issue that might severely limit the spectral efficiency and, definitely, the achievable capacity. Another drawback of rectangular pulses is related to their sensitivity to linear bandpass filtering. In order to avoid waveform corruption and subsequent ISI (Inter Symbol Interference), a very large system passband is required, say, e.g.: 5-10 times the baud-rate [10-12]. For the above reasons, the use of band-limited pulse shaping may be envisaged for broadband satellite applications. A well-known band-limited pulse is the raised cosine (RSC) [10]. RSC is commonly employed in satellite communications in combination with QAM (Quadrature Amplitude Modulation) or QPSK (Quadrature Phase-Shift Keying) modulation, implementing the so-called RSC-filtered QAM (or QPSK) [12]. RSC is intrinsically ISI-free (it fulfills Nyquist's conditions) and can be generated by means of digital FIR (Finite Impulse Response) filters. Moreover, it is much less sensitive to filtering than rectangular pulse. The main disadvantages of RSC are: a) unlimited pulse duration in time that may involve inter-pulse interference (IPI), in particular when the transmission rate is very high and b) very relevant envelope fluctuations of the RF (Radio Frequency) modulated signal resulting in high values of the Peak-to-Average-Power-Ratio (PAPR). As RF power amplifiers usually employed in W-band satellite connections (like Traveling Wave Tube Amplifiers – TWTA) efficiently work in nonlinear saturation zone, the transmitted signal can be severely affected by waveform corruption and ISI. As noted in [11], no ISI-free point can be observed in the eye-pattern diagram of the received RSC signal in the presence of nonlinear distortions. Therefore, the use of raised cosine in satellite communications, advisable from the spectral efficiency viewpoint, requires appropriate countermeasures against

nonlinear distortions.

The usual solution considered in satellite communications is to sacrifice power efficiency in order to avoid nonlinear distortion effects. This is realized by fixing the working point of the amplifier at the border of the linear zone of the AM/AM characteristic, introducing an input back-off (IBO) of the transmitted power [12][13].

In such a way, nonlinear distortions would be removed at the price of a substantial reduction of the power efficiency due to the resulting Output Back-Off (OBO).

Alternative solutions are based on pre-distortion circuits like clipping and filtering (employed e.g. in multicarrier modulations [14]) and envelope equalization [15]. Both solutions rely on a deliberate envelope compression that may involve a noticeable increase of Bit-Error-Rate (BER) at the receiver side. Adequate countermeasures in terms of increased-complexity baseband detection [14] and channel coding [15] have been considered in order to obtain acceptable BERs.

The necessity of sidelobe power reduction and constant envelope of the RF signal makes Gaussian Minimum Shift Keying (GMSK) modulation a feasible and theoretically favorable solution to W-band PHY-layer design. GMSK is a modulation technique widely employed in terrestrial telephony [16], in particular in the GSM standard. More recently, GMSK found some interesting applications in satellite communications ([17] [18]). GMSK is derived by Minimum Shift Keying (MSK) signal that is a form of Offset-QPSK signaling with sinusoidal pulse shaping [10]. MSK is characterized by constant envelope (being a frequency modulation) and sidelobes considerably lower than QPSK, but at the expense of a significantly larger main lobe [12]. For GMSK, unmodulated data (rectangular-shaped pulses) are processed by a LPF filter, having Gaussian-shaped frequency response, before frequency modulation [10]. This filter greatly reduces the spectral sidelobes with

respect to MSK signals [10] [15]. The introduction of the Gaussian filter involves a decrease of efficiency due to the increase of ISI. Literature points out that a good compromise for relatively low sidelobes and tolerable ISI is given by a bandwidth of the Gaussian LPF that equals 0.3 times the bit-rate [10][15]. GMSK is characterized by a reduced spectral efficiency with respect to QPSK and RSC-filtered QAM/QPSK. In fact, the main lobe of GMSK is about 1.5 times larger than the main lobe of usual (not filtered) QPSK and 2 times larger (and even more) than that of RSC-filtered QPSK [10]. This fact should be adequately taken into account when dealing with finite and non-ideal bandpass characteristics of satellite systems. In Tab. 1 a summary of pros and cons of state-of-the-art modulation techniques applied to a broadband satellite scenario is shown.

Table 1. Comparison of efficiency of state-of-the-art modulation solutions against satellite W-band PHY-layer design issues

	SPECTRAL EFFICIENCY	SIDE-LOBE POWER REDUCTION (W/O DISTORTIONS)	SENSIBILITY TO NON-IDEAL BAND-LIMITED FILTERING	RESILIENCE AGAINST NON-LINEAR DISTORTIONS	ENERGY CONCENTRATION IN A FINITE TIME WINDOW (PULSE DURATION)
QAM (rectangular pulse)	Very bad	Very low	Very high	Optimal	Optimal
RSC-filtered QAM	Very good	Optimal	Low	Very low	Poor
GMSK	Fair	Very good	Relatively low	Optimal	Very good

In this work, we shall consider a non-conventional solution for radio interface of high-frequency broadband satellite communications, targeted at positively solving the tradeoff between finite pulse duration, spectral efficiency and envelope compactness. The leading concept underlying the proposed methodology is to avoid the sacrifice of power efficiency and spectral efficiency in order to limit distortion effects. In fact, power is an important resource in satellite communications and the need for efficient

use of available power increases with frequency, being power generation a major technological challenge for “beyond Ka-band” telecommunication systems.

The proposed modulation solution is based on Prolate Spheroidal Wave Functions (PSWFs) pulse waveforms, already considered in the framework of indoor Ultra-Wideband (UWB) terrestrial communications [19]. Such waveforms are characterized by optimal concentration of energy both in the time and frequency domain. It is known that it is not feasible to generate bandlimited signals in finite time, because of the time-frequency indetermination principle [10]. Slepian and Pollack demonstrated in [20] that defining α as the energy concentration in a time window T and β as the energy concentration in a finite bandwidth W (both T and W are assigned), the maximum attainable α and β are given by the largest eigenvalue of a Fredholm integral equation with sinc kernel, whose eigenfunctions are known as Prolate Spheroidal Wave Functions (PSWFs). PSWFs are fully programmable in length, size and spectral shape, since they are determined by the eigenvalues setting [20] [21]. Being the energy concentrated in the main spectral lobe, PSWF waveforms generally exhibit a relevant power reduction in secondary spectral lobes that can be adaptively shaped by tuning the generation parameters. This is the reason why PSWFs find many applications also in cognitive radios [21].

In order to fully exploit the favorable features of PSWFs in the considered broadband satellite scenario, we propose a radio interface design based on a 4-ary Pulse Shape Modulation (PSM), using 1st and 2nd order PSWFs as pulse waveforms. Such kind of modulation, introduced in [22], can be compared with RSC-filtered QAM (or RSC-filtered QPSK) in terms of spectral efficiency but, differently from RSC-filtered QAM, it is characterized by very low PAPR.

The comparison between 4-ary PSM, RSC-filtered QAM and GMSK is performed in

terms of: i) achievable spectral efficiency, ii) sidelobe power reduction, iii) sensibility to filtering, and iv) BER measured in a simulated W-band GEO satellite scenario related to broadband downlink transmission. Results in terms of link availability for specific satellite services (broadcast and high definition television, Internet browsing) will be shown as well. This last series of results is obtained by using estimated W-band attenuation sequences related to supplementary rain fading. Curves for channel BER vs. percentage of the operational time are plot for 4-ary PSM modulation, RSC-QAM modulation and GMSK modulation. Then, Forward Error Correction (FEC) coding is adequately dimensioned in order to obtain the expected BER values required by the considered applications. At the end of this analysis, the achievable net payload rate, normalized with respect to the RF signal bandwidth, is shown for all the different transmission solutions analyzed in the paper.

The rest of the paper is structured as follows: Section II focuses on the description of the W-band satellite link together with some main issues to be faced in the effective PHY-layer design, such as: link impairments, distortions, rain attenuation, W-band usage regulatory and spectrum management issues. Section III introduces the basic concepts underlying PSWF-based pulse shaping together with the 4-ary PSM modulation technique adopted for the considered W-band satellite system. The mathematical modeling of distortions and other link impairments are shown in Section IV. Experimental results are presented and discussed in Section V. Finally, paper conclusions are drawn in Section VI.

II. Broadband transmissions over W-band: link description, issues and channel impairments

A. Link description

In this paper, we focused our analysis on the forward downlink segment of a GEO W-band transmission system. This link is usually the most critical one because of many well-known reasons; among which the most important are the quality of the user receiver (which is in general lower than that of the earth station devices due to necessity of keeping the user-terminal cost-competitive) and the power consumption limitations on the satellite, which require the HPA (High Power Amplifier) to work very close to saturation. Moreover, the forward downlink segment is the most bandwidth-demanding, because it is devoted to large data downloads by residential users, as shown in the pictorial scheme of Fig.1. The earth station can be regarded as a “broadband communication centre” that provides to remote residential sites both broadcast services (TV and HDTV) and TCP-based services (e.g.: Internet browsing). Both the forward uplink segment and the forward downlink segment are implemented in W-band. Without loss of generality, the GEO satellite is assumed to be regenerative.

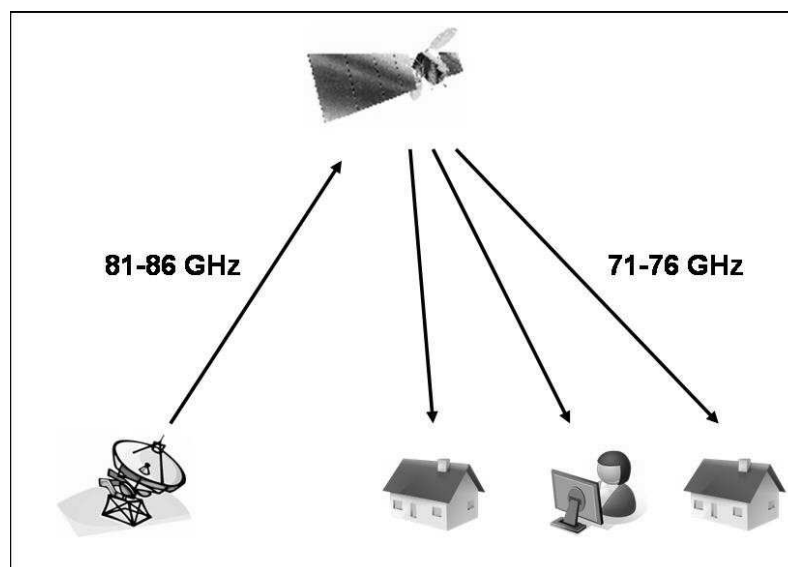


Figure 1. W-band GEO satellite link (pictorial scheme).

In the present scenario, we fixed the channel data rate of the link equal to 1 Gbit/sec, in order to provide the opportunity of the “gigabit connectivity” to the service-oriented satellite system of Fig.1. The net payload rate will be less than 1 Gbit/sec, as we shall assume the use of channel coding in order to comply with BER requirements of different satellite transmission applications. Therefore, we shall compare results achieved by different pulse shaping techniques not only in terms of bit-error-rates, but also in terms of achievable net payload rates (see Section V).

B. Main issues on W-band satellite communications

W-band satellite communication is a novel and very interesting field of research that needs to be deeply investigated in order to design the proper radio interface.

W-band satellite communication shows some interesting features that can be very attractive both for commercial and dual-use applications, such as: good interference protection, through the use of very narrow spot beams, and high anti jammer protection, due to wider theoretically available spreading bandwidth. In the present paper, we do not consider signal spreading, leaving this interesting topic as matter for future research.

Antennas operating in this band have a higher directivity than antennas (of the same size) operating at lower frequencies, so the interference between adjacent satellite position is reduced; moreover this high directivity makes it possible to use high-gain spot beam satellite antennas, increasing down-link power flux density and saving satellite power (one of the most important platform resources); in addition high

frequency reuse can be realised, exploiting the bandwidth resource in a very efficient way.

Another important improvement provided by EHF is the reduction of RF hardware equipment. This makes the use of W-band particularly attractive with respect to the realisation of portable terminals and smaller satellite payloads, for example in the context of space exploration, where mass and size are among the most important mission drivers. On the other hand, W-band telecommunications technologies are currently under development. Some equipment has been already used for satellite Earth observation applications (i.e.: cloud profiling) and terrestrial radar applications, but they need to be slightly changed to be used for TLC applications while other critical components need to be completely developed. In this framework, one of the most critical issues is power generation; therefore very low HPA back-off level shall be used.

The most relevant sources of signal degradation in a W-band geostationary satellite link are amplifiers, oscillators and frequency Doppler. The HPA must be powerful enough to overcome high path losses typical of EHF GEO satellite transmissions. HPAs exhibit two relevant distortions that can severely affect the received signal: nonlinear distortion due to the saturating characteristic of the amplifier and linear bandpass distortion due to non-ideal bandpass characterization of RF amplifier circuitry. The nonlinear AM/AM characteristic may involve a noticeable alteration of the modulated signal envelope [23]. On the other hand, the nonlinear AM/PM characteristic introduces a phase drift that varies with the input signal amplitude [23]. Linear bandpass distortion consists of a frequency-selective alteration of the modulated signal amplitude, due to the “bell-shaped” bandpass characteristics of HPAs, together with a phase distortion mainly due to the frequency-selective group

delay of front-end filters [12]. The degradation of the transmitted signal due to linear and nonlinear distortions causes Inter-Symbol-Interference and significant phase jitter at the receiver. Moreover, spectral re-growth involved by nonlinear effects [12] will cause adjacent channel interference and violation of spectral mask requirements, as shown in [13].

With a commonly-accepted degree of approximation (see e.g. [8]), we can say that nonlinear distortion of the satellite modem chain is imposed by HPAs, linear amplitude distortion is mostly imposed by amplifiers (HPAs and LNAs, Low Noise Amplifiers) and, finally, linear group delay distortion is mainly imposed by front-end filters. In Section IV, we shall detail the methodologies for modeling and simulation of linear and nonlinear link distortions.

EHF satellite links are also affected by relevant frequency uncertainties. High-frequency oscillators, present both in the up-conversion and in the down-conversion stages, are not ideal and can exhibit high levels of phase noise. Consequently, we have a frequency instability that may impact the performance of the carrier recovery loop in terms of longer acquisition time, frequency mistracking, and may produce a residual phase jitter that significantly lowers BER performance.

C. W-Band rain fading modeling and estimation

One of the main drawbacks of W-band satellite links is the large atmospheric fade experienced when rainfall occurs along the path, in addition to the gaseous atmospheric absorption by oxygen and water vapour; this attenuation shall be carefully taken into account in W-band link testing simulation. In particular, rain fading time-series shall be synthesized.

In the literature, different methodologies are used for rain attenuation time-series synthesis for EHF satellite links [24], including the spectral model, synthetic storm techniques, the two-sample model, and N -state Markov chain models. These models are used for links operating in Ka and Q/V bands, being obtained from empirical measurements performed during scientific satellite missions [25]. Most of these models cannot be effectively used for W band rain attenuation time-series synthesis because they need data from empirical measurements as input; as a matter of fact, no attenuation record database is available for the W band satellite link. In this framework, the N -state Markov chain model could be considered as one of the best choices in order to achieve some credible results. This model does not require empirical measurements; the only inputs are the link characteristics (including rain attenuation cumulative distribution function), the geographical meteorological data of the ground station, and the fade slope characteristics. The N -state Markov chain model [26] is divided into two sub-models. The first one is referred as macroscopic model and provides a time series consisting of two possible states: “rain” and “no rain”. The second part of the model is the so-called microscopic model. Its task is to fill the boxes of “rain” states obtained from the macroscopic model. The microscopic model provides the short-term dynamic behavior of rain attenuation (using the information provided by the fade slope distribution). In order to generate complete long-term time-series the two time-series obtained from the previous parts have to be combined. The transition probabilities of the N -state Markov chain model are based on ITU-R Recommendation [26]. The input data requested to run the model are the geometrical configuration (satellite and Earth station locations), radiowave characteristics (frequency and polarization) and the climatological parameters being given by ITU-R radio-meteorological maps [27]. Minor changes have been made to

the model in order to adapt it to W band, using frequency scaling techniques. In Fig. 2 an example of a W band rain attenuation time series is shown (1 day). The link characteristics used as input for the model are: operating frequency $f=76$ GHz, elevation angle $\theta=41.5^\circ$, maximum attenuation $A_{max}=80$ dB, threshold attenuation $A_{min}=2$ dB, low-pass scintillation filter cutoff frequency $f_B=0.035$ Hz. The Earth station is located in Rome (latitude 42° , longitude 12°).

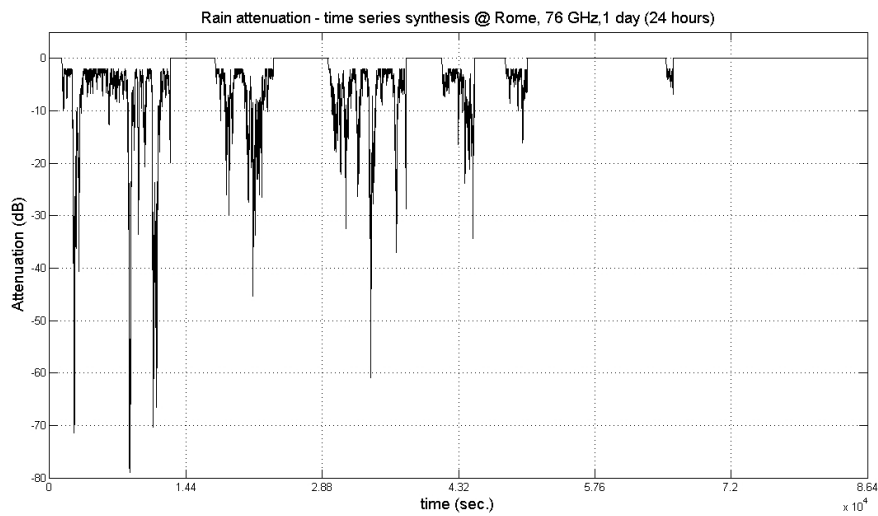


Figure 2. Example of W-band synthesized rain attenuation time-series (duration: 24 hours).

Starting from attenuation values reported in Fig. 2, we derived in Fig. 3 the corresponding cumulative distribution of estimated rain fading. On the horizontal axis, percentage of service time (24 hours) is reported, ranging from 63% to 99%. The values reported on the vertical axis represent the maximum attenuation value encountered during the related percentage of service time. For instance, we can read from the curve that the rain attenuation will be lower than 4dB for 80% of the service time and lower than 14dB for the 95% of the service time. The curve of cumulative rain fading of Fig.3 can provide some preliminary indications about the link

availability.

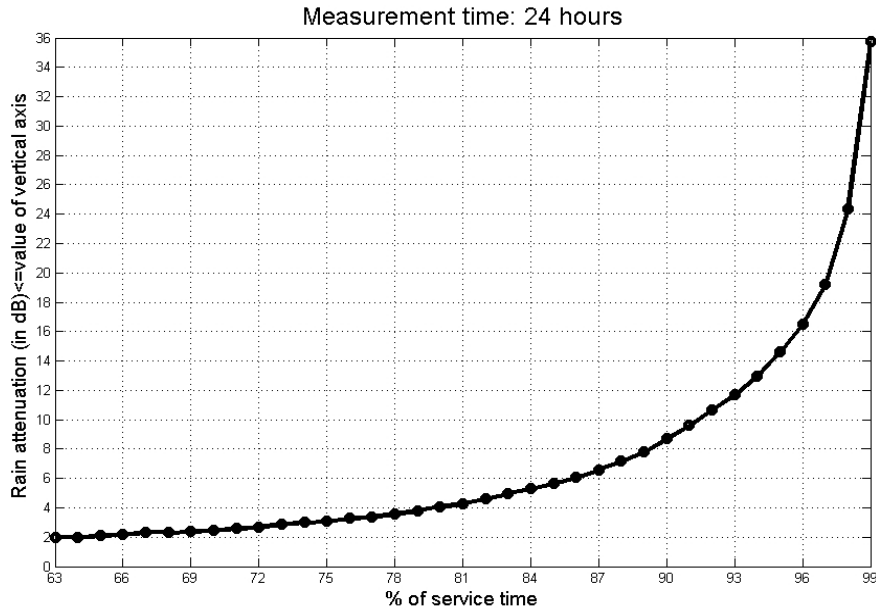


Figure 3. Cumulative distribution function of the additional rain attenuation.

However, in evaluating link availability, transmission impairments mentioned in subsection II.B should be carefully taken into account. The tie between PHY-layer distortions and rain fading will be considered in subsection V.C, where results in terms of link availability and net payload rate will be shown for specific communication services delivered to residential customers.

D. W-band GEO link regulations and spectrum management issues

Currently, the millimeter wave spectrum beyond 70 GHz is a very important field of research for broadband communications, both terrestrial and satellite. The regulations on the use of this part of the spectrum are not so strict, both for Europe and United States. A so-called “light licensing regime” has been adopted for terrestrial radio applications of W-band. The updated requirements for frequency filing in the 71-76

GHz, 81-86 GHz and 92-95 GHz have been published by FCC in 2005 [28]. The position and characteristics of the stations are recorded on a database on a first-in-first-served basis, with responsibility for subsequent users to ensure the compatibility with previously notified stations. “Light licensing” can be practically used due to the highly directional “pencil-beam” that can be obtained using W-band antennas. This allows the design of systems that can operate in proximity to one another causing very low (or no) interference.

FCC regulatory (that is only mentioned as a reference – being not related to satellite link) does not consider in details specific issues of side-lobe power and ACI limitations. This is due to the fact that the use of W-band in satellite links is really in the early experimental phase and, as previously mentioned, the interference analysis is in charge of the user before registration. Anyway, we can refer to some recommendations issued by international standardization associations like ETSI and related to lower frequencies. One of these recommendations [29], dealing with interactive satellite terminals in geostationary orbit operating at 11/12 GHz (earth to space) and 29/30 GHz (space to earth), contains a frequency mask where side-lobe emissions should be down 27.3 dB relative to the maximum of the power spectral density in the nominal signal bandwidth. This regulation may be regarded as a valuable reference also for the W-band satellite transmission case, when the spectral efficiency of the different PHY-layer solutions will be analyzed and compared in Section III.

III. PSWF-Based Modulation/Demodulation Section

A. Description of waveform generation, modulator and demodulator

As clearly shown in Section II, high-data rate satellite links operating in W-band can be affected by relevant impairments that may strongly influence performance in terms of link availability. In this paper, we consider an innovative transmission approach able to limit the effects of distortion and increase the link availability in broadband services. Such an approach relies on the use of pulse shaping based on Prolate Spheroidal Wave Function (PSWFs). PSWFs were first studied by D. Slepian and H. Pollack (Bell Labs) in 1961 [20]. The fundamental concept standing at the basis of PSWFs is to concentrate the energy of the pulse in limited regions, both in time and frequency domains. The starting point is the definition of a spectral bandpass mask, centered at a given intermediate frequency f_I (in this paper f_I is supposed to be equal to 5GHz) i.e.:

$$H_M(f) = \begin{cases} 1, & f_I - W/2 < |f| < f_I + W/2 \\ 0, & \text{otherwise} \end{cases} \quad (1)$$

The pulse design problem is reduced to “how to find a time-limited pulse waveform, given the desired spectral mask $H_M(f)$ and its corresponding impulse response $h_M(t)$ ”. In order to design such kind of waveforms, let’s define an arbitrary time-limited pulse kernel $\psi_M(t)$ as:

$$\psi_M(t) = \begin{cases} p_M(t), & |t| < T/2 \\ 0, & \text{otherwise} \end{cases} \quad (2)$$

Then, we send the kernel function $\psi_M(t)$ through the target filter $h_M(t)$. Let the filter output be defined as follows [20]:

$$\lambda_M \psi_M(t) = \int_{-T/2}^{T/2} \psi_M(\tau) h_M(t-\tau) d\tau \quad (3)$$

It can be demonstrated (omitting mathematical details for sake of brevity) that the

solution of (3) can be obtained by solving the following equation [20]:

$$\lambda_M \psi_M(t) = \int_{-T/2}^{T/2} \psi_M(\tau) \frac{\sin[W(t-\tau)]}{t-\tau} d\tau \quad (4)$$

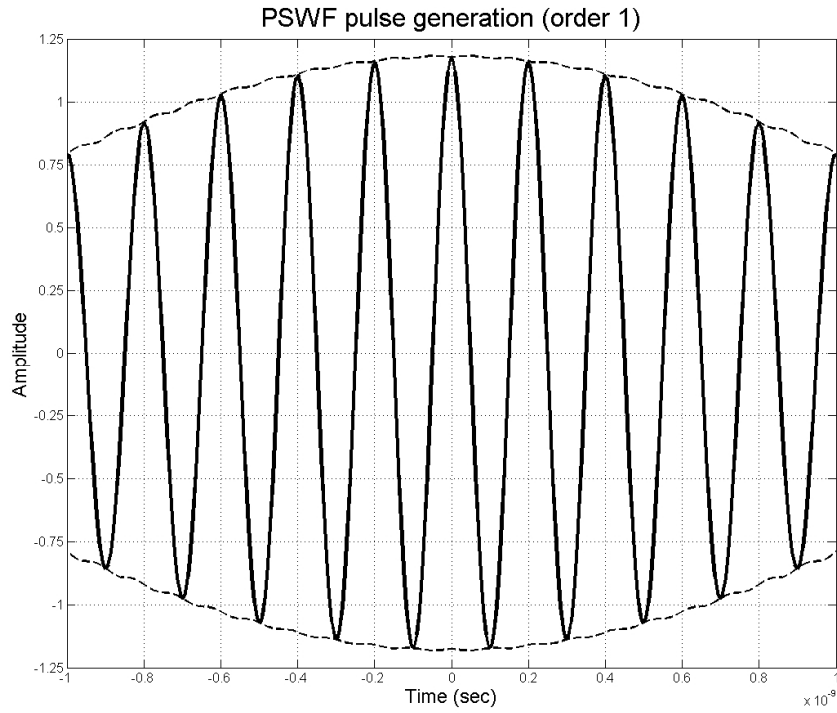
$0 < \lambda_M < 1$ is the energy concentration factor of $\psi_M(t)$. It denotes the percentage of pulse energy that lies in the time slot of duration T . Solutions of (4) are very difficult to find in closed form. A discretization algorithm can be employed to obtain a numerical solution. By sampling at a rate of N samples/pulsewidth we can represent (4) in the following form:

$$\lambda_M \psi_M(n) = \sum_{m=-N/2}^{N/2} \psi_M(m) h_M(n-m) \quad n = -\frac{N}{2} \dots \frac{N}{2} \quad (5)$$

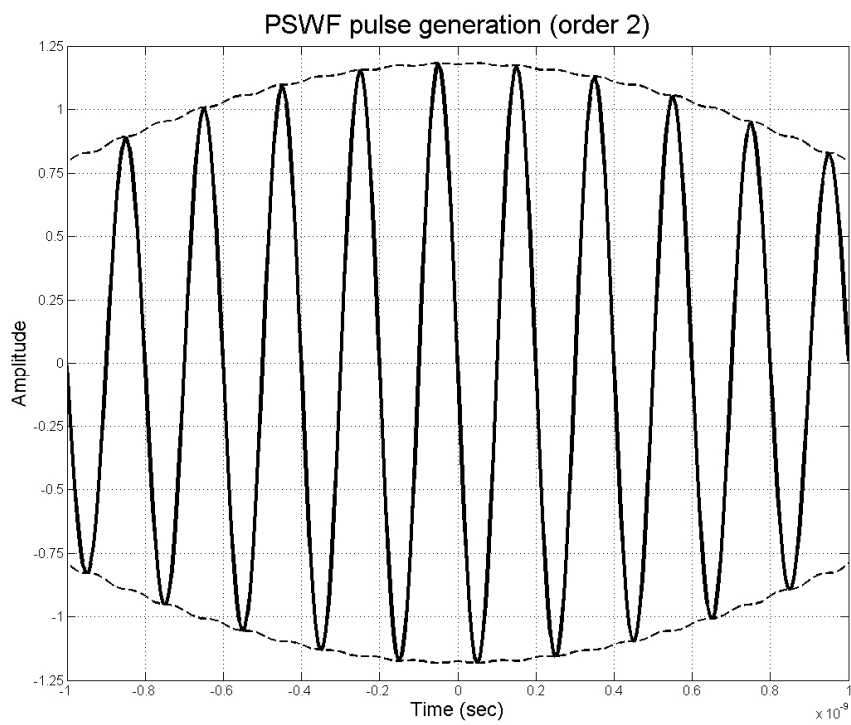
Expressing into matrix form, the numerical solution of (4) can be found by means of eigenvalue decomposition [20]. In particular, by solving (5), we shall obtain the eigenvectors $\underline{\psi}_1, \underline{\psi}_2, \dots, \underline{\psi}_n$ corresponding to the different eigenvalues. $\psi_n(t)$ is the n -th order PSWF [20]. PSWFs are characterized by some interesting properties, i.e.:

- pulse waveforms of different orders are mutually orthogonal;
- pulse width and pulse bandwidth can be simultaneously controlled to match with arbitrary spectral masks (adaptive pulse shaping);
- pulse width and bandwidth are the same for all orders;
- by definition, PSWFs exhibit an optimized tradeoff between concentration of the energy in a finite time window and in a finite bandwidth: this means that the resulting modulated signal is characterized by “almost finite” pulse duration and, at the same time, “almost limited” bandwidth.

Moreover, it is very interesting to note that PSWFs of order 1 and order 2 are characterized by surprising envelope compactness, as shown in Figs. 4 (a) and (b).



(a)



(b)

Figure 4. (a): 1st order PSWF waveform, (b): 2nd order PSWF waveform (the dashed lines represent the complex envelopes).

This fact suggests the use of a PSWF-based modulation scheme fully exploiting such a good property, i.e.: the 4-ary Pulse Shape Modulation (PSM) proposed in [22]. Such a modulation is characterized by the same spectral efficiency as QAM/QPSK and “almost constant” envelope [22]. By this, the effect of HPA nonlinearity should be drastically reduced both in terms of waveform corruption and in terms of spectral regrowth. Another strength of 4-ary PSM, applied in the considered broadband satellite scenario, is related to the spectral compactness that is intrinsic to PSWFs. On one hand, the high concentration of energy on the main spectral lobe should provide a reduced sensibility to filtering. On the other hand, the reduced side-lobe level should meet the strict regulations on satellite spectrum management that shall be issued as soon as W-band will become a bandwidth resource concretely available for commercial services. These are the motivations that inspired us to experiment 4-ary PSM in the W-band “gigabit” satellite scenario. Expected results are in terms of: a) increased resilience against nonlinear effects with respect to RSC-filtered QAM, obtained without sacrificing power efficiency, and: b) increased normalized efficiency in terms of bit/s transmitted per Hz with respect to GMSK due to the reduced bandwidth occupation.

The generic M -ary PSM scheme is detailed in [22]. Furthermore, the mapping of different 4-ary symbols into four amplitude levels modulating the two waveforms of Fig.4 has been shown in Tab.2.

Table 2. 4-ary PSM symbol mapping

SYMBOL	1ST ORDER PSWF (PULSE 1)	2ND ORDER PSWF (PULSE 2)
00	-pulse 1	-pulse 2
01	-pulse1	pulse 2
11	pulse 1	pulse 2
10	pulse 1	-pulse 2

In the real transmission system, 1st and 2nd order PSWFs would be generated at intermediate frequency of 5GHz and the corresponding 4-ary PSM signal is frequency upconverted in W-band (76GHz), amplified and transmitted to the earth terminal. The demodulator is based on a coherent scheme using two matched filters (see [22] for further details), each one matched to the single orthogonal waveform used to transmit the data bitstream. The carrier recovery loop proposed by Cabric et al. in [31] for 60GHz terrestrial UWB applications, has been also considered in our satellite EHF scenario for what concerns 4-ary PSM and RSC-filtered QAM. This circuit is based on a phase rotator and on a decision-directed phase error detector. It exhibits a good tradeoff between computational efficiency and robustness against frequency uncertainties typical of EHF 60 GHz terrestrial applications [31].

B. RF-modulated signal analysis in frequency and time domain

In this sub-section, an analysis of the 4-ary PSM signal in time and frequency domain is presented, in order to introduce the potential advantages that can be obtained by the proposed PSWF-based modulation scheme with respect to RSC-filtered QAM, non-filtered QAM and GMSK in the considered satellite scenario. A comparison in terms of bandwidth occupation, sidelobe power level and PAPR level will be shown in the following.

The basic parameter governing adaptive PSWF time-frequency pulse shaping is λ_M . Fixing the symbol duration T , we can adaptively set the bandwidth occupied by the PSWF-based modulated signal. Dually, fixing the bandwidth W , we can set the symbol duration T . Using a 4-ary PSM modulation, assuming a channel data rate equal to 1Gbit/s, the signaling interval T is fixed to 2 nsec. In order to reach the

maximum spectral efficiency (i.e.: 2 bit/s/Hz), the bandwidth W is set to 500MHz. Using such settings, we obtain $\lambda_M = 0.78$, meaning that the 78% of the pulse energy is concentrated in the signaling interval. Therefore, windowing the pulse as required in (3), we generate out-of-band components. Indeed, the bandwidth occupied by the modulated PSM signal is larger than 500MHz. The analysis of the different modulated signals in the frequency domain is shown in Fig.5, where the power spectrums related to: a) 4-ary PSM, b) QAM with rectangular pulses, c) RSC-filtered QAM (roll-off factor equal to 0.5) and d) GMSK modulations respectively are compared for a channel data-rate of 1 Gbit/s.

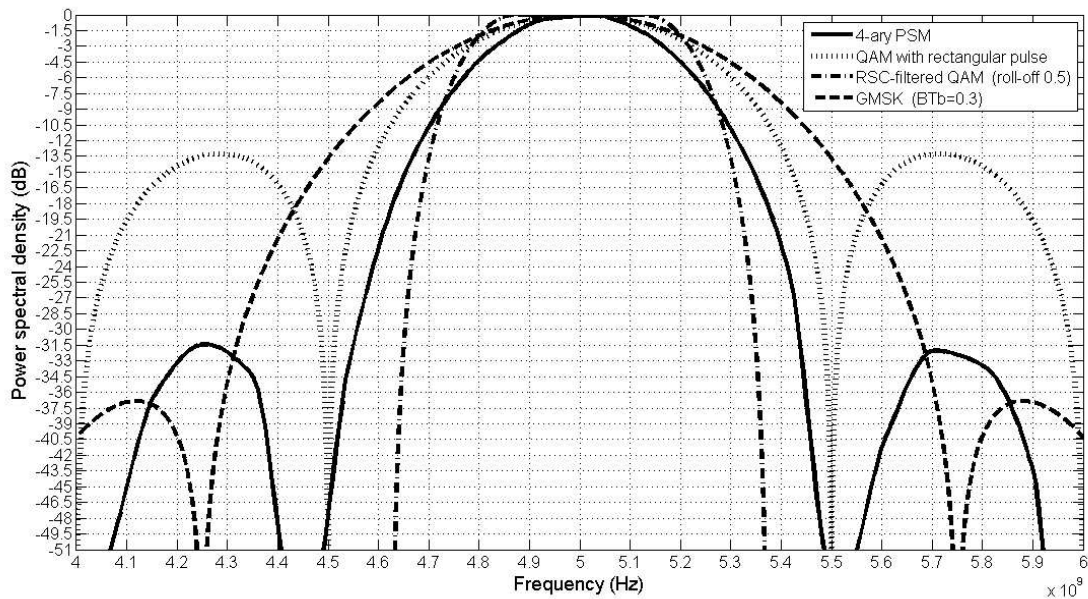


Figure 5. Power spectral densities of the modulated signals: PSWF-based 4-ary PSM (solid line), QAM with rectangular pulse shaping (pointed line) RSC-filtered QAM with roll-off 0.5 (dash-dotted line), and GMSK (dashed line). Plotted values are expressed in dB.

It is clear from Fig.5 that RSC-filtered QAM is optimal with respect to the sidelobe power reduction, being RSC pulse bandlimited (main lobe bandwidth equal to 750

MHz). However, we can observe that even band-unlimited 4-ary PSM exhibits a strongly reduced sidelobe power (31.5dB lower than the main lobe peak power) that is slightly larger than that one of GMSK (36.75dB lower than the main lobe peak power). It should be said that both sidelobe power levels are fully compliant with the spectral mask of [29]. However, the main lobe of the GMSK signal is about 1.4 times larger than the corresponding one of the 4-ary PSM signal. On the other hand, the peak power level of the secondary lobe of the QAM using rectangular pulse shaping is 13.5dB lower than the main lobe peak power that is clearly not compliant with the spectral mask of [29].

A first estimation of the RF bandwidth of the PSM modulated signal can be derived by Fig.5, considering bandwidth occupancy 16dB down from maximum. Such a bandwidth is approximately equal to 700 MHz, which is rather close to that one of RSC-filtered QAM (i.e.: 750MHz) and substantially reduced with respect to GMSK one, which was estimated, on the basis of the above-mentioned criterion, as approximately equal to 1 GHz. All these values will be taken into account when the sensibility of the considered pulse waveforms to nonideal bandpass filtering will be assessed in sect. V.

The main advantage of PSWFs with respect to RSC is surely related to the reduced PAPR that is the well-known indicator of envelope compactness. Tab. 3, reporting PAPR values for all the pulse waveforms considered in this section, shows that the lower bound on PAPR (i.e.: 0 dB) is reached by QPSK/QAM with rectangular pulse shaping and GMSK. These last ones are indeed constant envelope modulations. It is interesting to note that PAPR of 4-ary PSM signal (i.e.: 1.04 dB) is quite close to the theoretical lower bound, while RSC-QAM signals exhibit much higher PAPRs (i.e.: 3,22 dB and 3.80 dB respectively), as already pointed out by literature [12].

Table 3. PAPR of modulated signals using different pulse shaping.

PULSE SHAPING	PAPR VALUE
RSC-filtered QAM (roll-off 0.5)	3.22 dB
RSC-filtered QAM (roll-off 0.35)	3.80 dB
4-ary PSM	1.04 dB
GMSK, QAM	0dB

The envelope compactness of 4-ary PSM is confirmed by the waveforms depicted in Fig. 4 (a) and (b). One can note from Figs. 4 that the modulated signal envelope ranges from 0.8 and 1.12. On the basis of the above considerations, one can understand that the choice of PSWFs may represent a very good compromise between envelope compactness and spectral efficiency. In a broadband EHF satellite transmission scenario, like the one depicted in Sect. II, such features seem to be very favorable.

IV. Mathematical modeling of W-band satellite link impairments

In this section, we shall describe the mathematical model of link impairments and distortions affecting a W-band satellite connection.

Rain fading is translated into a supplementary attenuation term, whose cumulative distribution is given in Fig. 3. Therefore, the bit-error-rate performance measured in presence of rain fading is to be interpreted as the worst-case BER during the given percentage of service time.

As far as amplifier distortions are concerned, we considered a TWTA with the AM/AM and AM/PM characteristics modeled by using Saleh's memory-less model [23]. Saleh's model is based on a class of nonlinear functions of the following kind:

$$f(r) = \frac{\kappa r^n}{(1 + \zeta r^2)^{\nu}} \quad (6)$$

where n and ν are assigned integer values, κ and ζ are derived from the experimental data obtained by the Least-Square (LS) curve fitting method proposed in [23], and r is the signal amplitude. The functions belonging to this class are general-purpose, in the sense that they can be used both for AM/AM and AM/PM characteristics. In order to derive a credible nonlinear amplifier simulation, we started from some real AM/AM and AM/PM characteristics contained in confidential data sheets related to commercial TWTA devices working in W-band. Therefore, we selected the values of n and ν more suitable to fit the real amplifier curves and, finally, we derived the values of κ and ζ fitting the experimental data. The resulting AM/AM and AM/PM characteristics used for our simulations have been depicted in Fig.6 and 7, respectively. It is easy to note that the AM/AM characteristic has been normalized in order to make easier simulation tasks.

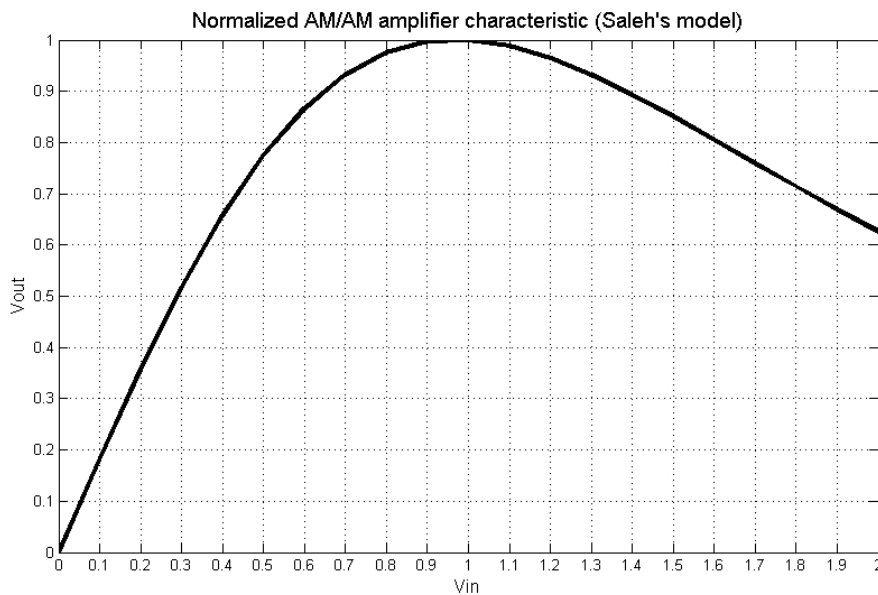


Figure 6. Simulated AM/AM characteristic of the High-Power Amplifier.

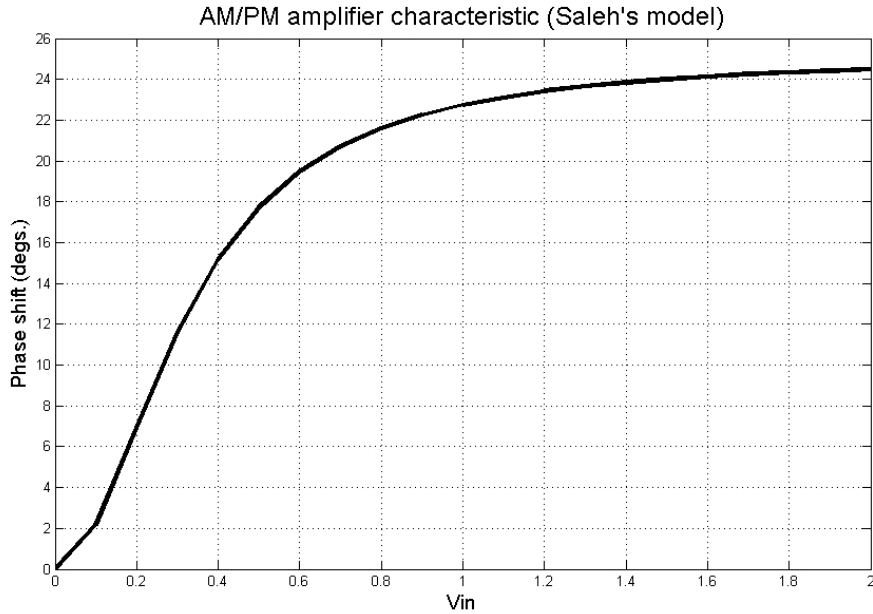


Figure 7. Simulated AM/PM characteristic of the High-Power Amplifier.

An analog parametric filter design with controllable shaping has been used in order to model non-ideal bandpass behavior of the satellite link. For sake of simplicity in parameterization and shaping control, classical bandpass *Butterworth filters*, as described in [10], have been employed to model such a kind of distortion. Butterworth filters are characterized by a magnitude response that is maximally flat in the passband and monotonic overall. The transfer function of a bandpass Butterworth filter is given by [10]:

$$H_{BP}(\omega) = \frac{1}{1 + j \left(\frac{\omega - \omega_c}{\omega_r} \right)^n} \quad (7)$$

where n is the *filter order* [10], and ω_r is the *cutoff (radian) frequency*. Also in this case, we considered data related to bandpass characteristic of real RF devices working in W-band (power amplifiers, front-end filters, etc.), and we simulated a credible bandpass amplitude and phase pattern by using Butterworth transfer functions. The

total non-ideal bandpass amplitude and phase characteristic of the satellite link is shown in Fig.8 and 9 respectively, centered at a frequency of 76GHz. The curves of Figs.8-9 have been obtained for a filter passband equal to 700 MHz. In our simulations, passband will be regarded as a free parameter.

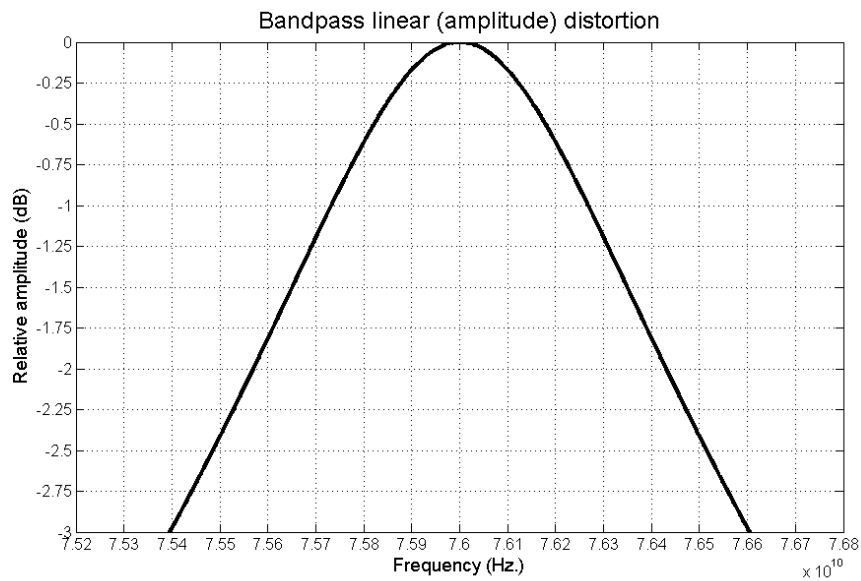


Figure 8. Simulated amplitude linear distortion of the W-band satellite link (passband: 700 MHz).

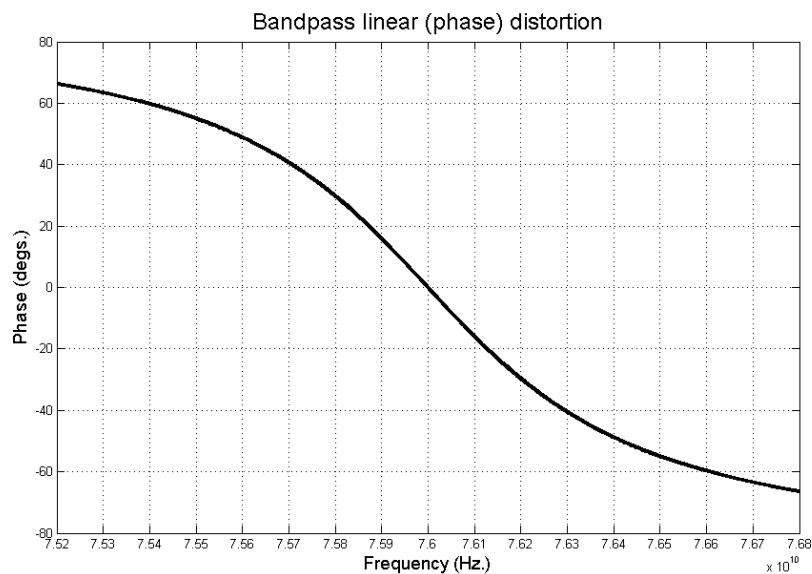


Figure 9. Simulated phase linear distortion of the W-band satellite link (passband: 700 MHz).

As far as the mathematical modeling of phase noise is concerned, we have considered the simple parametric model proposed in [30]. In particular, it is assumed that the baseband power spectral density (PSD) of the phase-noise is given by:

$$S_{\phi}(f) = \Lambda f_c^2 / f^2 \quad (8)$$

Λ being a constant measured on the basis of the ratio of the single-sideband (SSB) phase-noise power to the power in the fundamental (expressed in dBc/Hz), for a certain frequency offset. By setting the parameter Λ , different realization of phase noise characterized by different standard deviations σ_{ϕ} can be obtained. In Fig.10, a phase noise sequence realization is shown ($\sigma_{\phi}=15^{\circ}$). Carrier recovery must work in the presence of a high Doppler shift with the disturbance of phase-noise that adds unpredictable frequency shifts. W-band GEO connections are characterized by an estimated Doppler shift equal to 90 kHz. Such a value is much lower than Doppler shift of W-band LEO connections (it may reach 2.5 MHz [8]). Therefore, as opposed to the LEO case, Doppler estimation and compensation may not be required in GEO applications. In this paper, Doppler shift is assumed to be uncompensated and frequency tracking is performed entirely by the carrier recovery loop.

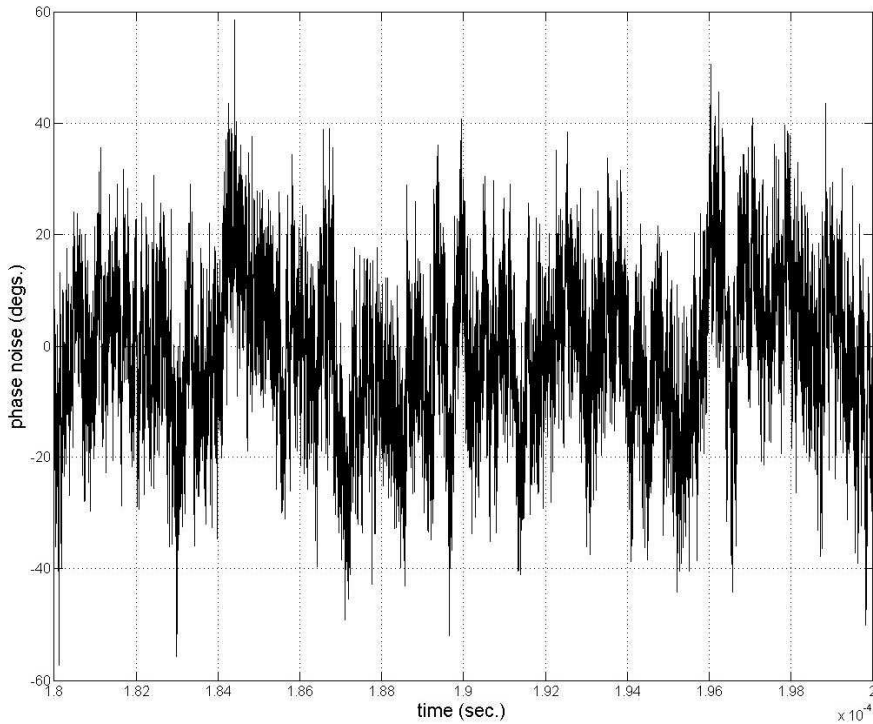


Figure 10. Sample realization of the simulated phase-noise process (standard deviation: 15°).

V. Experimental Results

A. Computationally-efficient simulation of the W-band satellite GEO link

In order to compare the different transmission solutions mentioned in Section III (4-ary PSM RSC-filtered QAM and GMSK), we performed intensive simulations using MATLAB-SIMULINK (version 7.1) environment. The end-to-end downlink transmission chain has been simulated in IF (Intermediate Frequency) (10GHz) following the same strategy adopted in [8], and [9]. The reason of this choice is the need to reduce the computation time that would be too high if we simulated the chain at the real RF value of 76 GHz. Such a major computational effort would be really useless. In fact, all link distortions are substantially frequency-invariant. Phase-noise is added straightforward and parameterized in terms of standard deviation. As

mentioned in Section III, PSFWs are generated at an initial IF of 5 GHz. Afterwards, in the simulated system; the IF is upshifted to 10 GHz (instead of 76 GHz). GMSK and RSC-filtered QAM signals have been generated in the baseband domain and, afterwards, upshifted to the same IF frequency chosen for the 4-ary PSM (i.e.: 10 GHz). As far as GMSK demodulation is concerned, the usual orthogonal coherent detector, also typical of MSK [16], has been considered. The state-of-the-art carrier recovery loop designed by De Buda [32] for frequency shift keying modulations has been employed in order to ensure coherent demodulation. It should be said that such a solution has been explicitly suggested in [16], as it supports implementation with conventional digital logic circuits that is very advisable for mobile and satellite communications systems.

The link budget of the forward downlink connection is reported in Tab. 4. It is compliant with the guidelines contained in [6], taking into account the constraints of the available technologies for W-band communications, mostly in terms of available transmission power. Assuming a channel data rate of 1Gbit/s, the link budget of Tab.4 would ensure a per-bit signal-to-noise ratio (namely: E_b/N_0) at the output of the demodulator equal to 19.2dB. If we consider the ideal case of AWGN channel, Shannon's capacity theorem tells us that a spectral efficiency equal to 6.4 bit/s/Hz would be theoretically achievable. We shall show that a PHY-layer design based on PSWF pulse shaping can substantially increase link capacity in the presence of all the impairments described in Sect. II and mathematically modeled in Sect. IV.

Table 4. W-band link budget for 1Gbit/s downlink GEO connection of Fig.1.

PARAMETER	NUMERICAL VALUE
Frequency	76 GHz
RF-power	20 dBW
TX gain	60 dB
TX terminal EIRP	80 dBW
Pointing loss	0.6 dB
Free-space loss	221.78 dB
RX terminal gain	56.2 dB
RX noise temperature	29.6 dB°K
RX G/T	26.6 dB/°K
Depointing loss	1 dB

In the following, we shall discuss two distinct series of simulation results that demonstrate the effectiveness of the proposed PHY-layer design methodology based on PSWF waveforms:

- Effects of linear, nonlinear distortions and phase noise on link performance in terms of bit-error-rate vs. per-bit signal-to-noise ratio (subsection V.B);
- Results in terms of link availability (expressed in terms of percentage of service time), considering performance requirements of most commercial satellite services, such as: broadcast and high definition television (HDTV), and Satellite Internet (subsection V.C).

Finally, in subsection V.D some potential challenges arising in the practical implementation of PSWF-based pulse-shaped modulations will be discussed.

B. Performance in presence of link distortions and phase noise

As far as link distortion effects are concerned, BER results assuming an infinite passband of the TX/RX system (i.e.: absence of linear distortions) are shown in Fig.11. The theoretical BER bounds for QAM and GMSK are for the ideal AWGN channel. Ideal GMSK is characterized by a loss of BER performance of 0.5dB with

respect to QAM (as already observed in [16]). It is easy to see that 4-ary PSM signals can be transmitted at the saturation point of the AM/AM characteristic without appreciable performance losses with respect to the ideal QAM case. Such result can be easily understood by considering amplifier characteristic of Fig.6 and the reduced PAPR yielded by 4-ary PSM evidenced both by values of Tab. 3 and by PSWF waveforms envelope depicted in Fig.4 (a) and (b). The same is observed for GMSK, but this is expected as GMSK is a constant-envelope modulation. As expected, RSC-filtered QAM exhibits very bad BER performance when the amplifier works in saturation without any back-off. A relevant performance improvement is obtained for RSC by introducing a back-off of the transmitted power up to the limit of the linear zone. Curves for RSC-filtered QAM are shown in Fig.11 with OBO=3.3 dB for roll-off=0.5 and OBO=4.3 dB for roll-off=0.35, respectively. Such a choice can be regarded as that one guaranteeing the best power efficiency for the simulated AM/AM characteristic of Fig.6. However, the noticeable performance improvement obtained by power back-off is paid in terms of a sacrifice of power efficiency with respect to the ideal QAM BER curve, i.e.: 2.5dB for roll-off=0.5 and 3.25 dB for roll-off=0.35, respectively.

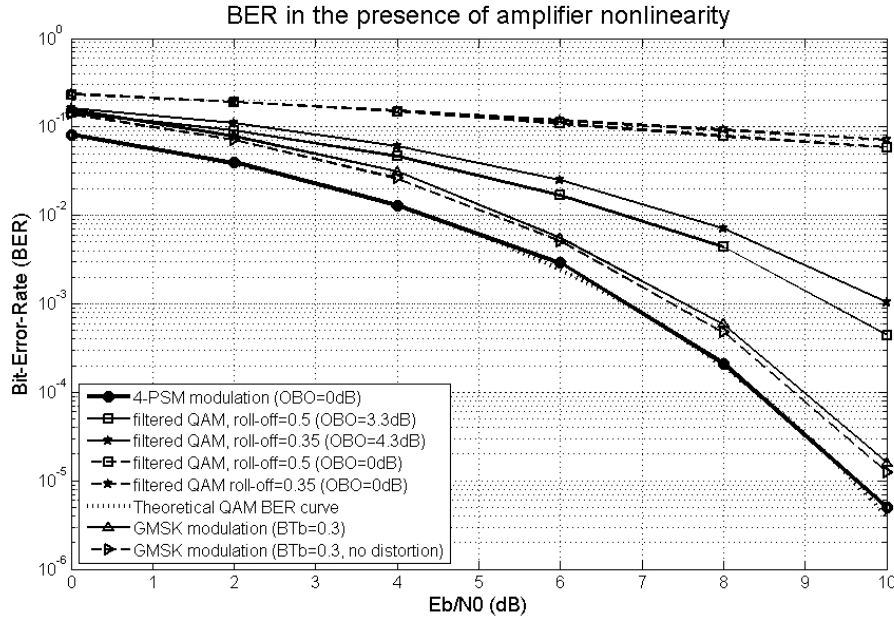


Figure 11. BER vs. E_b/N_0 in the presence of nonlinear distortion only.

Simulation results dealing with the effects of linear distortion are shown in Fig.12. The comparison has been made among 4-ary PSM, RSC-filtered QAM and GMSK. In fact, non-filtered QAM requires a very large system passband in order to avoid distortion and ISI and, for this reason, the comparison with spectrally-efficient modulation schemes is not reasonable. “Passband” is used here to mean the 3dB-bandwidth of the equivalent Butterworth filter emulating such non-ideal behavior. Considering a passband of linear distortion equal to 700MHz (see Section III), we can see that 4-ary PSM performance is affected by a loss of 2.25dB with respect to the infinite passband case. Such a value is compliant with the requirements of satellite standards considering 2-2.5dB as acceptable values for losses due to linear distortion (see e.g. [8]). A slightly-reduced performance loss (i.e.: 1.5dB) is experimented by RSC-filtered QAM signal, passing through a 3dB bandwidth equal to the signal (limited) bandwidth (i.e.: 750 MHz for roll-off 0.5 and 675 for roll-off 0.35). Such performance loss is caused by residual ISI involved by the deformation of the spectral

RSC lobe due to non-ideal filtering. It is worth noting that the two BER curves corresponding to the different roll-offs are almost coincident, meaning that the effect of linear filtering is substantially independent on the RSC spectral shape. As far as performance of GMSK in the presence of linear distortion is concerned, we can observe a performance loss (2.5dB) quite similar to that one yielded by 4-ary PSM under equivalent filtering conditions.

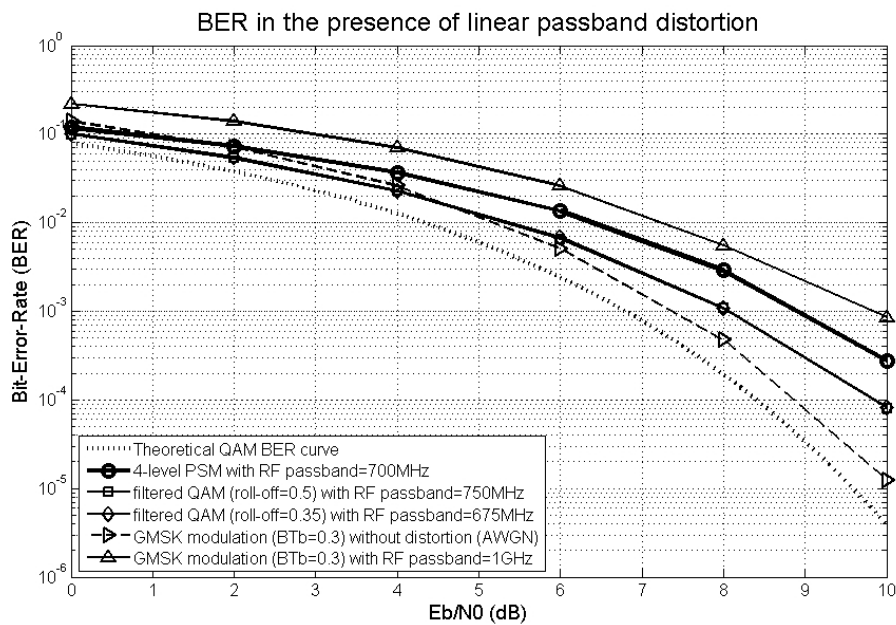


Figure 12. BER vs. E_b/N_0 in the presence of linear distortion only.

The combined effect of linear and nonlinear distortion is shown in Fig.13. Only curves related to transmission with power back-off have been shown for RSC-filtered QAM. We can say that the adoption of PSWF waveforms instead of RSC can be advantageous in the presence of heavy RF non-linear distortions, as the HPA can be fully exploited at its maximum efficiency. The impact of linear distortion is in favor of RSC that would become more suitable in the case of using linear or quasi-linear amplifiers. It should be said that the use of linear power amplifier is not frequent in

broadband satellite communications and proper distortion compensation mechanisms should be considered. On the other hand, GMSK performance is slightly degraded with respect to 4-ary PSM (the loss measured in Fig.13 is about 1dB), and noticeably improved with respect to RSC-filtered QAM employed with OBO. It should be noted that GMSK requires an increased bandwidth expense with respect to all the modulation schemes assessed in this section.

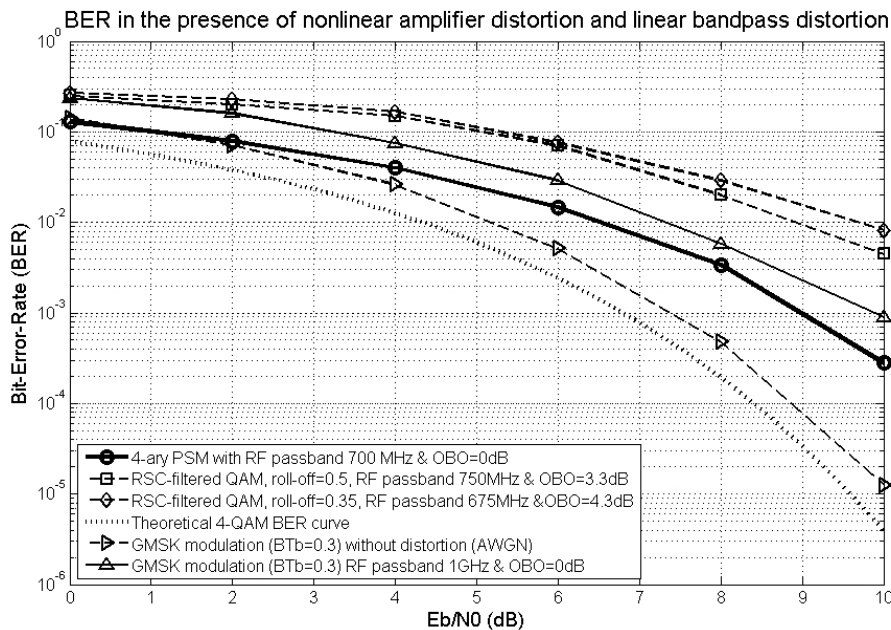


Figure 13. BER vs. E_b/N_0 in the presence both of nonlinear and linear distortions.

The additional performance loss involved by the presence of phase noise has been shown in Fig.14, for $\sigma_\phi=10^\circ$ and $\sigma_\phi=15^\circ$ respectively. Results have been shown only for PSWF and GMSK modulations. RSC-filtered QAM shows a behavior of the carrier recovery loop very similar to that one exhibited by 4-ary PSM, being this loop substantially independent on the selected pulse shaping. Linear and nonlinear distortion effects have been taken into account also in this simulation series, with the

same parameterization considered in Fig. 13. In Fig.14, the lower performance bounds are represented by the 4-ary PSM and GMSK BER curves obtained in the absence of phase-noise, but in the presence of all other link distortions. One can note that the additional performance loss due to phase noise becomes very relevant when $\sigma_\phi = 15^\circ$, both in the 4-ary PSM case and in the GMSK one. Other available simulation results, not shown in Fig.14 for sake of graphical clarity, show that the trend of all BER curves related to all considered modulations is towards an irreducible error-floor as far as σ_ϕ becomes larger than 15° . This is the effect of the residual phase jitter, measured at the output of the carrier recovery loop after convergence to the expected frequency. [33]. On the other hand, the impact of phase noise on transmission quality becomes almost irrelevant for $\sigma_\phi < 7^\circ$. Performance losses of 1.5dB, measured for 4-ary PSM, and 2dB, measured for GMSK, (both values are related to phase noise with $\sigma_\phi = 10^\circ$) are still tolerable (see [8] [9]).

Note that we did not report results for $E_b/N_0 < 5\text{dB}$, as for such values of signal-to-noise ratio, the carrier recovery loop of [31] doesn't converge. On the other hand, the carrier recovery loop adopted by GMSK is able to converge for $E_b/N_0 > 2.5\text{dB}$. This means that GMSK might provide very limited link availability also for very low SNRs (as better evidenced in the next subsection).

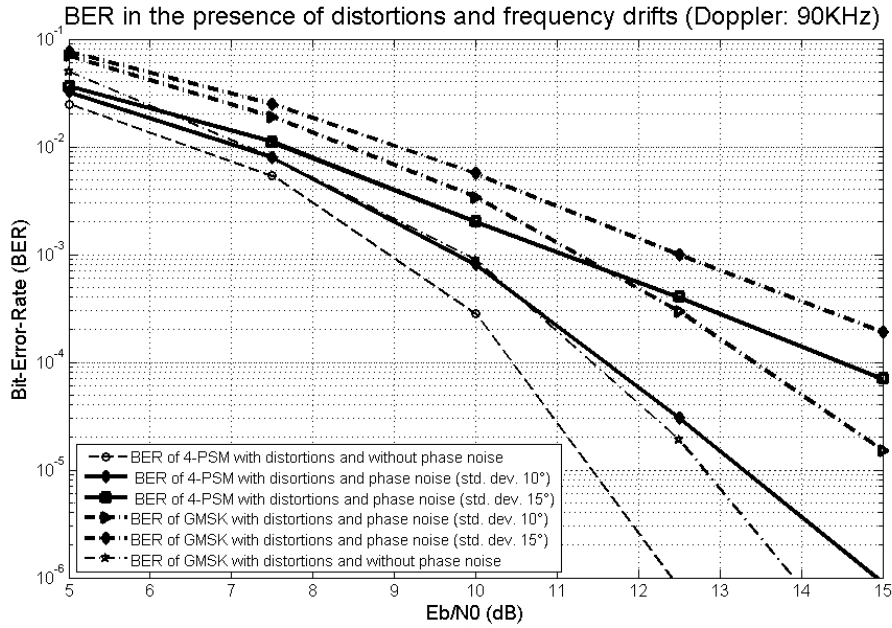


Figure 14. BER vs. E_b/N_0 in the presence of link distortions (linear and nonlinear) and phase-noise.

C. Results in terms of link availability targeted to the provision of specific services

In satellite connections, it is of paramount importance to test the link availability, i.e. the percentage of operational time during which the link performance does not go down an “out-of-order” threshold depending on the provided service. Starting from the link budget of Tab. 4 and from the cumulative distribution function of the channel attenuation shown in Fig.3, we plot in Fig. 15 the curves of the available link bit-error-rate in the presence of the rain attenuation. As the rain attenuation is given in cumulative way, BER values shown in the vertical axis should be regarded as the highest ones during the percentage of service time shown in the horizontal axis. All link distortions described in Section II and mathematically modeled in section IV have been considered in this series of simulations. The standard deviation of phase noise has been set to the maximum value assuring an acceptable performance loss ($\sigma_\phi = 10^\circ$). In order to quantify the link availability, we assume that the satellite link

becomes “out-of-service” when channel BER is higher than 10^{-1} : in this case Reed-Solomon (RS) or convolutional FEC coding may fail to correct channel errors. Under this assumption, one can see in Fig.15 that the link availability is guaranteed at least for 94% of the operational time for all the considered pulse-shaped modulation techniques. As far as 4-ary PSM and RSC-filtered QAM are considered, the link goes “out-of-service” for the remaining 6% of the operational time, as the signal-to-noise ratio goes under the threshold required by the carrier recovery to converge (i.e.: 5dB). As previously mentioned, the carrier recovery loop of GMSK converges for lower SNRs, therefore the link availability would be theoretically guaranteed for 95% of the operational time. From curves of Fig.15, it can be noted that 4-ary PSM BER performance is better than that of GMSK when link availability equal to 94% is considered. The value of 94% can be regarded as the nominal link availability of the considered W-band satellite connection. On the other hand, the performance improvement yielded both by 4-ary PSM and GMSK with respect to RSC-filtered QAM is clearly evident. The same values of OBO indicated in Figs.11 and 13 have been considered also in this series of simulations related to RSC-filtered QAM, in order to obtain meaningful BER values. It should be noted that GMSK can achieve BER performance quite close to that of 4-ary PSM and better than that of RSC-filtered QAM with OBO. But the RF bandwidth occupied by GMSK is larger than that one of the other assessed pulse-shaped modulation schemes (with the exception of non-filtered QAM). This fact, already underlined in Section III, involves some considerations that should be carefully taken into account in optimizing W-band satellite PHY-layer design.

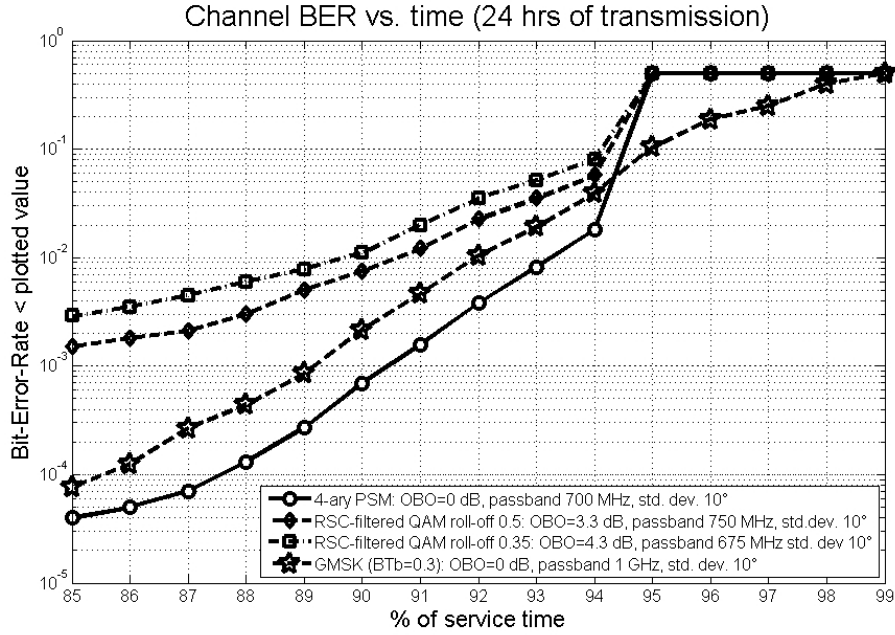


Figure 15. Channel BER vs. percentage of operational time achieved by simulations for the attenuation time series of Fig.2 (24 hours of transmission).

In such a perspective, the reduced channel BER and the increased spectral efficiency yielded by 4-ary PSM would allow to efficiently exploit the available bandwidth resources in order to increase the net payload rate and, definitely, increase the quality of service perceived by residential users. In particular, the performance improvement yielded by 4-ary PSM might have a great impact in dimensioning channel coding needed to obtain the bit-error-rate required by satellite networking applications. For this reason, we shall show a last series of results concerning with the available net payload rate achieved by some well-known commercial satellite services. In order to make a fair comparison among different modulation solutions, we shall normalize the available net payload rate with respect to the estimated RF signal bandwidth (namely: *normalized efficiency*). In our analysis, we consider a RS coding and we assess coding performance by means of the usual lower bound expression for bit-error probability P_B achieved at the output of the RS channel decoder [34], i.e.:

$$P_B \cong \frac{1}{n} \sum_{i=t+1}^n i \binom{n}{i} P_c^i (1 - P_c)^{n-i} \quad (9)$$

where P_c is the channel bit-error probability, t denotes the number of errors that can be corrected in an (n, k) block code. In a RS code $t = (n-k)/2$ [34].

We compare the code rates needed to ensure BER values typical of: a) MPEG-2 broadcast TV applications (BER 10^{-6} [35]), b) Internet browsing supported by satellite TCP/IP (BER 10^{-8} [36]), c) HDTV by satellite (BER 10^{-11} [37]). In Tabs.5-8 code rates, net payload rates and normalized efficiency are shown for 4-ary PSM, RSC-filtered QAM (roll-off 0.5 and 0.35), and GMSK respectively. One can note that the use of PSWF waveforms increases the normalized efficiency and, definitely, to exploit more efficiently the wide available bandwidth. The improvement in normalized efficiency achieved by 4-ary PSM with respect to RSC-filtered QAM is quantified in about 23% for the MPEG-2 TV broadcast, 27% for the satellite Internet services, and even 36% for satellite HDTV services. On the other hand, the normalized efficiency of GMSK (see Tab. 8) is substantially penalized by the larger RF bandwidth occupied by the modulated signal, both with respect to 4-ary PSM and of RSC-filtered QAM (the percentage of normalized efficiency reduction with respect to 4-ary PSM is on average equal to 38%).

Table 5. Available code rates (for 94% of operational time), net payload rates and normalized efficiency achieved by 4-ary PSM modulation.

	RS CODING	NET PAYLOAD RATE	NORMALIZED EFFICIENCY
MPEG-2 TV	(129,107)	829 Mb/s	1,18 b/s/Hz
Internet on sat	(127,101)	795 Mb/s	1.13 b/s/Hz
HDTV	(137,103)	750 Mb/s	1.07 b/s/Hz

Table 6. Available code rates (for 94% of operational time), net payload rates and normalized efficiency achieved by RSC-filtered QAM modulation (roll-off: 0.5).

	RS CODING	NET PAYLOAD RATE	NORMALIZED EFFICIENCY
MPEG-2 TV	(131,89)	679 Mb/s	0.91 b/s/Hz
Internet on sat	(125,77)	616 Mb/s	0.82 b/s/Hz
HDTV	(129,71)	550 Mb/s	0.73 b/s/Hz

Table 7. Available code rates (for 94% of operational time), net payload rates and normalized efficiency achieved by RSC-filtered QAM modulation (roll-off: 0.35).

	RS CODING	NET PAYLOAD RATE	NORMALIZED EFFICIENCY
MPEG-2 TV	(133,81)	609 Mb/s	0.90 b/s/Hz
Internet on sat	(135,75)	556 Mb/s	0.82 b/s/Hz
HDTV	(127,59)	464 Mb/s	0.69 b/s/Hz

Table 8. Available code rates (for 94% of operational time), net payload rates and normalized efficiency achieved by GMSK modulation ($BT_b=0.3$).

	RS CODING	NET PAYLOAD RATE	NORMALIZED EFFICIENCY
MPEG-2 TV	(137,103)	752 Mb/s	0.75 b/s/Hz
Internet on sat	(153,107)	700 Mb/s	0.70 b/s/Hz
HDTV	(145,93)	641 Mb/s	0.64 b/s/Hz

It should be noted that GMSK may provide link availability of 95%, but with very low normalized efficiency. In fact, in order to reach the expected quality of service for 95% of the service time, the following RS codes would be required: a) RS(155,113) for MPEG-2 TV, b) RS(127,55) for Internet browsing and c) RS(137,51) for HDTV. The corresponding values of normalized efficiency would be: 0.487 bit/s/Hz, 0.433 bit/s/Hz, and 0.372 bit/s/Hz respectively. This means that the increase of link availability, theoretically achievable by GMSK, might be actually obtained at the expense of heavy redundancy added to the transmitted message and, consequently, of a very inefficient bandwidth resource usage.

D. Practical implementation issues

As claimed in [19] and [21], the implementation of a preliminary cognitive UWB radio is a reachable goal today thanks to the existence of programmable pulse waveform generators. However, the realization of an “arbitrary” UWB waveform is still quite challenging due to the limitations of current digital processing hardware. In fact, A/D and D/A converters are not fast enough to be capable of implementing adaptive pulse shaping. Therefore, the basic implementation issues related to the generation of pulse waveforms like PSWF should be carefully investigated. In [21], a feasible solution for PSWF generation is proposed based on subsampling. Subsampling is typically employed in software radio applications in order to avoid very high sampling frequencies [38]. Subsampling introduces aliasing; therefore out-of-band noise rejection filters have been proposed in order to counteract aliasing effects [38]. Alternatively, we can assume to tolerate an acceptable amount of aliasing without adding complexity to front-end hardware. It is stated in [21] that a resolution of 4 bit/sample can decrease the total number of samples per waveform until 64 samples/pulse, while maintaining the basic spectral characteristics of the generated PSWF-based signal. Following the approach of [21], a sampling frequency of 32 GHz would be required to the D/A converter in order to generate the IF-equivalent 4-ary PSM signal. Such a frequency is not apparently reachable by state-of-the-art devices. For this reason, further downsampling should be forecast at the price of introducing anti-aliasing filters. This will be challenging matter of investigation as soon as the practical implementation of the UWB-like solutions for broadband satellite communications will be considered.

VI. Conclusions

In this paper, advanced pulse-shaped modulation techniques based on Prolate Spheroidal Wave Functions (PSWF) (recently proposed in the framework of short-range UWB communications) have been considered in a broadband W-band satellite scenario, with the aim of reaching the “gigabit connectivity”. In particular, 4-ary PSM modulation using PSWF produces an “almost constant” envelope RF signal, characterized by increased spectral efficiency. The proposed pulse shaping methodology is then compared with state-of-the-art waveforms adopted in satellite communications in terms of a) efficiency in spectrum management in terms of bandwidth occupation and power reduction of secondary lobes, and b) robustness against the effects of linear and nonlinear distortions. 4-ary PSM modulation demonstrates its favorable characteristics in the presence of amplifier distortions (linear and nonlinear) with an evident performance improvement with respect to RSC-filtered QAM employed with power back-off. Compared to a constant envelope modulation like GMSK, 4-ary PSM provides better BER performance and reduced bandwidth occupancy. Furthermore, 4-ary PSM is characterized by a sidelobe power fully compliant with commonly-used satellite spectral masks. Phase noise should be reasonably limited in any case, as its impact on system performance may be relevant. Thanks to such good properties, PSWF can offer augmented service availability with increased net payload rates and better efficiency, in terms of bandwidth usage, with respect to “traditional” modulation solutions. For such reasons, PSWF-based pulse shaping can be regarded as valuable candidates to support future broadband connections in W-band. Future work might concern with the study of a feasible full-

digital PSWF generator, coping with the actual limitations of digital signal processing hardware. Another interesting point might consider the extension of the study to multi-level PSM modulation. In such a case, higher-order PSWFs must be employed in order to modulate the bitstream. Envelope compactness of PSM signal would not be longer guaranteed, but the comparison with RSC-filtered M-QAM modulation might be still in favor of 4-ary PSM.

VII. Acknowledgements

This work has been partially supported by the Italian Ministry of University and Scientific Research (MIUR), under the framework of SALICE research project (project code: COFIN 2007RFTYY7_002). Authors wish to thank Dr. M. Menapace of Space Engineering (Italy) for his valuable help in collecting experimental results and Prof. G. Dalla Betta of University of Trento (Italy) for his valuable suggestions related to hardware implementation issues.

References

- [1] M. Ibnkahla, Q.M. Rahaman, A.Y. Sulyman, H.A. Al-Asady, J. Yuan, and A. Safwat, "High-Speed Satellite Mobile Communications: Technologies and Challenges", *Proceedings of the IEEE*, Vol. 92, No. 2, Feb. 2004, pp. 312-339.
- [2] J. Farserotu, and R. Prasad, "A Survey of Future Broadband Multimedia Satellite Systems, Issues and Trends", *IEEE Comm. Mag.*, June 2000, pp. 128-133.
- [3] S. De Fina, M. Ruggieri, and A. V. Bosisio, "Exploitation of the W-band for High-Capacity Satellite Communications", *IEEE Trans. on AES*, vol. 39, no. 1; January 2003, pp. 82-93.

- [4] L.J. Ippolito, “*Millimeter Wave Propagation: Spectrum Management Implications*”, FCC Bulletin No. 70, Washington D.C.: July 1997.
- [5] M.Ruggieri, S.De Fina, M.Pratesi, A.Salome’, E.Saggese, C.Bonifazi, “The W-band Data Collection Experiment of the DAVID Mission”, *IEEE Transactions on AES*, Vol.38 n.4, Oct. 2002, pp.1377-1387.
- [6] A. Jebril, M. Lucente, M. Ruggieri, and T. Rossi, “WAVE – A new mission in W band”, *Proc. of 2005 IEEE Aerospace Conf.*, Big Sky (MT), March 5-12, 2005, paper n. 1007.
- [7] M. Lucente, T. Rossi, A. Jebril, M. Ruggieri, A. Iera, A. Molinaro, S. Pulitanò, C. Sacchi, and L. Zuliani, “Experimental Missions in W-Band: a Small LEO Satellite Approach”, *IEEE Systems Journal*, vol.2, no.1, March. 2008, pp. 90-102.
- [8] C. Sacchi, G. Gera, and C. Regazzoni, “W-band Physical Layer Design Issues in the Context of the DAVID-DCE Experiment”, *Int. Jour. of Satellite Communications and Networking*, Vol. 22, No. 2, March-April 2004, pp. 193-215.
- [9] C. Sacchi, and A. Grigorova, “Use of Trellis-Coded Modulation for Gigabit/sec Transmissions over W-Band Satellite Links”, *Proc. of 2006 IEEE Aerospace Conf.*, Big Sky (MT), March 4-11 2006, available on CD-ROM.
- [10] L.W. Couch, II, “*Digital and Analog Communication Systems*” (7th edition), Pearson – Prentice Hall, Upper Saddle River (NJ): 2007.
- [11] W.L. Martin, and T.M. Nguyen, “*CCSDS-SFCG Efficient Modulation Methods Study: A comparison of Modulation Schemes, Phase 2: Spectrum Shaping*”, CCSDS Tech. Rep. August 1994.
- [12] S. Turrò (ed.), “*Satellite Communication Systems Design*”, Plenum Press, New York: 1993.

- [13] J.L. Fikart, and B. Kocay, “Cost Effective Operating Power Specification of Ka-Band MMICS for Multimedia Satellite Interactive Terminals”, *Proc. of 1999 IEEE MTT-S Symposium on Technologies for Wireless Applications*, 21-24 Feb. 1999, pp. 247-252.
- [14] R. Dinis, and A. Gusmão, “A Class of Nonlinear Signal-Processing Schemes for Bandwidth-Efficient OFDM Transmission with Low Envelope Fluctuations”, *IEEE Trans. Commun.*, vol. 52, no.11, pp. 2009-2018, Nov. 2004.
- [15] M. Tomlinson, and M. Ambroze, “Power and Bandwidth Efficient Modulation and Coding for Small Satellite Communication Terminals”, *Proc. of IEEE 2002 Internat. Conf. on Communications (ICC’02)*, New York, Apr.28-May 2, 2002, pp. 2943-2946.
- [16] K. Murota, and K. Hirade, “GMSK Modulation for Digital Mobile Telephony”, *IEEE Trans. on Comm.*, vol. COM-29, no.7, July 1981, pp.1044-1050.
- [17] M. Rice, T. Oliphant, O. Haddadin, and W. McIntire, “Estimation Technique for GMSK using Linear Detectors in Satellite Communications”, *IEEE Trans. on AES*, vol.43, no.4, Oct. 2007, pp. 1484-1495.
- [18] K. Tsai, T. Oyang, J. Phan, C.C. Yang, and N. Schneier, “Gaussian Minimum Shift Keying Modulator”, *Proc. of IEEE Aerospace Conf. 2000*, Big Sky (MT), 18-25 March 2000, vol. 5, pp. 235-241.
- [19] L. Yang, and G.B. Giannakis, “Ultra-Wideband Communications – An idea whose time has come”, *IEEE Signal. Process. Mag.*, Nov. 2004, pp. 27-54.
- [20] D. Slepian, and H.O. Pollak “Prolate Spheroidal Wave Functions, Fourier Analysis and Uncertainty”, *I. Bell System Tech. J.*, vol. 40, 1961, pp. 43-64.

- [21] H. Zhang, X. Zhou, K.Y. Yazdandoost, and I. Chlamtac, "Multiple Signal Waveforms Adaptation in Cognitive Ultra-Wideband Radio Evolution", *IEEE Journ. of Sel. Areas in Comm.*, vol. 24, no. 4, Apr. 2006, pp. 878-884.
- [22] K. Usuda, H. Zhang, and M. Nakagawa, "M-ary pulse shape modulation for PSWF-based UWB systems in multipath fading environment", *Proc. IEEE Globecom 2004 Conf.*, Dallas (TX), Nov.29- Dec. 4 2004, pp. 3498-3504.
- [23] A.A.M. Saleh, "Frequency-independent and frequency-dependent nonlinear models of TWT amplifiers," *IEEE Trans. Commun.*, vol-COM 29, no.11, pp. 1715-1720, Nov. 1981.
- [24] R. Polonio, C. Riva, "ITALSAT propagation experiment at 18.7, 39.6 and 49.5 GHz at Spino D'Adda: three years of CPA statistics", *IEEE Trans. on Antennas and Propagat.*, vol. 46, no. 5, May 1998, Pag.631-635.
- [25] J. Lemorton, L. Castanet, F. La coste, C. Riva, E. Matricciani, U.C. Fiebig, M. Van De Kamp, and A. Martellucci, "Development and validation of time-series synthesizers of rain attenuation for Ka-band and Q/V-band satellite communication systems", *Int. Jour. of Satellite Comm. and Networking*, Vol. 25, No. 5, Oct. 2007, pp. 575-601.
- [26] L. Castanet, T. Deloues, J. Lemorton, "Methodology to simulate long-term propagation time-series from the identification of attenuation periods filled with synthesized events", *Int. Workshop on Satellite Communications from Fade Mitigation to Service Provision*, Noordwijk (NL), May 2003.
- [27] ITU-R Recommendation P.1623, "*Prediction method of fade dynamics on Earth-space path*", Geneva (CH), March 2005.

- [28] "Memorandum Opinion and Order In the matter of Allocations and Service Rules for the 71-76 GHz, 81-86 GHz, and 92-95 GHz Bands", FCC 05-45, WT Docket No. 02-146, released March 3, 2005.
- [29] prEN 301 SIT V0.2.2 (1997-10), "Satellite Earth Station and Systems (SES), Satellite Interactive Terminals using satellites in geostationary orbit operating in the 11/12 GHz (space to earth) and 29/30GHz (earth to space) frequency bands"
- [30] K.S. Kundert, "Introduction to RF Simulation and Its Application", *IEEE Jour. of Solid-State Circ.*, vol. 34, no. 9, Sept. 1999, pp. 1298-1319.
- [31] D. Cabric, M.S.W Chen, D.A. Sobel, S. Wang J. Jang, and R. Brodersen, "Novel Radio Architectures for UWB, 60GHz and Cognitive Wireless Systems", *EURASIP Jour. on Wireless Comm. and Networking*, vol.2006, Article ID 17957, pp. 1-18.
- [32] R. De Buda, "Coherent Demodulation of Frequency Shift Keying with Low Deviation Ratio", *IEEE Trans. on Comm.*, vol. COM-20, no.6, June 1972, pp. 466-470.
- [33] M.C. Jeruchim, V. Balaban, M. Shammugan, "*Simulation of Communication Systems*", Kluwer Academic Publishers, Norwell (MA), 2000.
- [34] E. Biglieri, "*Coding for Wireless Channels*", Springer, New York: 2005.
- [35] Y. Hsu, Y. Cheng, C.J. Huang, and M.J. Sun, "MPEG-2 Spatial Scalable Coding Transport Stream Error Concealment for Satellite TV Broadcasting Using Ka-Band", *IEEE Trans on Broadcasting*, vol. 44, no. 2, June 1998, pp. 233-242.
- [36] Y. Chotikapong, and Z. Sun, "Evaluation of Application Performance for TCP/IP via Satellite Link", *IEE Sem. on Satellite Services and the Internet*, Feb 17, 2000, pp. 4/1-4/4.

- [37] T. Nakai, Y. Hatano, and T. Kasezawa, H. Ito, and M. Nishida, “Development of HDTV Digital Transmission System through Satellite”, *IEEE Trans on Consumer Electronics*, vol. 41, no. 3, August 1995, pp. 604-614.
- [38] M.R. Yuce, and W. Liu, “Alternative Wideband Front-End Architectures for Multi-Standard Software Radios”, *Proc. of 2004 IEEE Vehicular Technology Conf. (VTC-2004 fall)*, Los Angeles (CA), 26-29 Sept. 2004, vol.3, pp. 1968-1972.



Claudio Sacchi obtained the “Laurea” Degree in Electronic Engineering, and the Ph.D. in Space Science and Engineering at the University of Genoa (Italy) in 1992 and 2003, respectively. Since August 2002, Dr. Sacchi has been holding a position as assistant professor at the Faculty of Engineering of the University of Trento (Italy). The research interests of Dr. Sacchi are mainly focused on: wideband mobile and satellite transmission systems based on space, time and frequency diversity, MIMO systems, array processing, multi-rate and multi-access wireless communications (OFDMA, DS/CDMA, MC-CDMA), cross-layer PHY-MAC design, EHF broadband aerospace communications, software defined radio-based design of reconfigurable multi-standard terminals, wireless and satellite communications for emergency recovery applications, etc.

Claudio Sacchi is author and co-author of more than 60 papers published in international journals and conferences. He is associate editor of *IEEE COMMUNICATIONS LETTERS* and reviewer for international journals and magazines like: *IEEE TRANSACTIONS ON COMMUNICATIONS*, *IEEE TRANSACTIONS ON WIRELESS COMMUNICATIONS*, *IEEE TRANSACTIONS ON AEROSPACE AND ELECTRONIC SYSTEMS*, *IEEE TRANSACTIONS ON VEHICULAR TECHNOLOGY*, *IEEE COMMUNICATIONS MAGAZINE*, etc. Dr. Sacchi is member of the Organizing Committees and Technical Program Committees of international conferences like *IEEE ICIP*, *IEEE ICC*, *IEEE GLOBECOM*, *ACM-MOBIMEDIA*, etc. In 2008, he was co-chair of the 1st *IEEE Workshop on Exploitation of Higher Frequency Bands in Broadband Aerospace Communications (EHF-AEROCOMM)*, held in conjunction with *IEEE GLOBECOM 2008*. Furthermore, he was symposium co-chair at *IEEE GLOBECOM 2009 (Selected Areas on Communications Symposium: track Satellite and Space Communications)*. Claudio Sacchi is Senior Member of *IEEE (SM'07)*, member of the *IEEE Communications Society* and of the *IEEE AES Society*.



Tommaso Rossi received his University Degree in Telecommunications in 2002, MSc Degree in “Advanced Communications and Navigation Satellite Systems” in 2004 and Ph.D. in Telecommunications and Microelectronics in 2008 at the University of Rome “Tor Vergata” where he is currently an Assistant Professor (teaching Digital Signal Processing). He is a member of the Italian Space Agency WAVE (W-band Analysis and VERification) Project Technical Team, a feasibility study for W-band telecommunication payloads. He is part of the scientific team that is defining the TDP#5 payload embarked on ESA Alphasat satellite. He has been a technical member of the ESA research project on Flowers Constellations. He has been involved in European Space Agency “EDRS” (European Data-Relay Satellite System) project. His research activity is focused on Space Systems, EHF Satellite Telecommunications, Satellite and Inertial Navigation Systems, Digital Signal Processing and Satellite Constellations.



Marina Ruggieri graduated in Electronics engineering in 1984 at the University of Rome. She joined FACE-ITT and GTC-ITT (Roanoke, VA) in the High Frequency Division during (1985-1986); then a Research and Teaching Assistant at the University of Rome Tor-Vergata (1986-1991); Associate Professor in Telecommunications at the Univ. of L'Aquila (1991-1994). Since November 2000 she is Full Professor in Telecommunications at the University of Rome Tor-Vergata. In 1999 she was appointed member of the Board of Governors of the *IEEE AES Society*, and in 2005 has been also appointed director of *IEEE-AESS* operations in Italy and Western Europe. She is a

member of the Editorial Board of Wireless Personal Communications KLUWER. She is an author of more than 220 papers, on international journals/transactions and proceedings of international conferences, book chapters and books. She was awarded the 1990 Piero Fanti International Prize and was nominated for the Harry M. Mimmo Award in 1996 and the Cristoforo Colombo Award in 2002. Her research mainly concerns space communications and navigation systems (in particular satellites) as well as mobile and multimedia networks.



Fabrizio Granelli received the "Laurea" (M.Sc.) degree in Electronic Engineering from the University of Genoa, Italy, in 1997, with a thesis on video coding, awarded with the TELECOM Italy prize, and the Ph.D. in Telecommunications from the same university, in 2001. Since 2000 he is Assistant Professor in Telecommunications and Co-Founder of the Dept. of Information Engineering and Computer Science, University of Trento (Italy) and coordinator of the Networking Laboratory. In August 2004, he was visiting professor at the State University of Campinas (Brasil). He is author or co-author of more than 90 papers published in international journals, books and conferences. Dr. Granelli is guest-editor of ACM Journal on Mobile Networks and Applications, special issues on "WLAN Optimization at the MAC and Network Levels", "Ultra-Wide Band for Sensor Networks" and "Recent Advances in IEEE 802.11 WLANs: Protocols, Solutions and Future Directions". Dr. Granelli is General Vice-Chair and Founder of WICON'05, General Chair of CAMAD'06, and General Co-Chair and Founder of MOBILIGHT'09.

He is TPC Co-Chair of IEEE GLOBECOM 2007-2009 Symposia on "Communications QoS, Reliability and Performance Modeling" and of IEEE CAMAD'08. His main research activities are in the field of networking, with particular reference to network performance modeling, cross-layering, medium access control, wireless networks, cognitive radios and networks. He is Senior Member of IEEE, Chair of IEEE ComSoc Technical Committee on Communication Systems Integration and Modeling (CSIM) and Associate Editor of IEEE Communications Letters, IEEE Communications Surveys and Tutorials and International Journal on Communication Systems.